

BENEFIT OF AIRBORNE FULL WAVEFORM LIDAR FOR 3D SEGMENTATION AND CLASSIFICATION OF SINGLE TREES

Josef Reithberger, Scientific collaborator
Peter Krzystek, Professor
Department of Geographic Information Sciences
University of Applied Sciences Muenchen
80333 Munich, Germany
(josef.reithberger, krzystek)@hm.edu
Uwe Stilla, Professor
Photogrammetry and Remote Sensing, Technische Universitaet Muenchen
80290 Munich, Germany
stilla@tum.de

ABSTRACT

The paper demonstrates the advantage of full waveform LIDAR data for segmentation and classification of single trees. First, a new 3D segmentation technique is highlighted that detects single trees with an improved accuracy. The novel method uses the normalized cut segmentation and is combined with a special stem detection method. A subsequent classification identifies tree species using salient features that utilize the additional information the waveform decomposition extracts from the reflected laser signal. Experiments were conducted in the Bavarian Forest National Park with conventional first/last pulse and full waveform LIDAR data. The first/last pulse data result from a flight with the Falcon II system from TopoSys in leaf-on situation at a point density of 10 points/m². Full waveform data were captured with the Riegl LMS-Q560 system at a point density of 25 points/m² (leaf-off and leaf-on) and at a point density of 10 points/m² (leaf-on). The study results prove that the new 3D segmentation approach is capable of detecting small trees in the lower forest layer. This was practically impossible so far if tree segmentation techniques based on the canopy height model (CHM) were applied to LIDAR data. Compared to the standard watershed segmentation the combination of the stem detection method and the normalized cut segmentation performs better by 12%. In the lower forest layers the improvement is even more than 16%. Moreover, the experiments show clearly that the usage of full waveform data is superior to first/last pulse data. The unsupervised classification of deciduous and coniferous trees is in the best case 93%. If a supervised classification is applied the accuracy is slightly increased with 95%. Classification with first/last pulse data ends up with only 80% overall accuracy. Interestingly, it turns out that the point density has practical no impact on the segmentation and classification results.

Keywords: LIDAR, Analysis, Segmentation, Forestry, Vegetation

INTRODUCTION

Commercial laser scanning technology has been pushed to a new level by fast electronic devices that render possible to record the entire laser pulse echo as a function of time. The recorded signal – a result of the interaction of the laser beam with one or several objects – is usually referred to as the waveform. Since 2004, new so-called full waveform small footprint LIDAR systems are available on the market such as the Riegl LMS-Q560 (same instrument as the Harrier 56 from Toposys) or the ALTM 3100 from Optech, which has the option for full waveform recording (see details Mallet et al., 2008). Since LIDAR penetrates vegetation the expectations are rather high that this technology will push new methods for the analysis of forest structures.

At least two possible ways are promising. The first one deals either with the single raw waveforms or overall waveforms accumulated from single waveforms in a working space (e.g. single tree). Since the waveforms are a function of tree parameters (e.g. age, tree species, height, crown diameter) measured waveforms could be compared with the theoretical model. Moreover, the tree parameters could even be adapted to real measurements by optimizing techniques. For instance, Koetz (2006) inverts a radiative model proposed by Sun et al. (2000) to adjust optical and structural parameters of the vegetation. Recently, Morsdorf et al. (2008) reports on a multi-spectral full waveform

simulator which uses the tree model PROSPECT and models the single laser beam with a ray tracing approach. A second strategy for waveform analysis in forest areas is to extract the inherent information of the waveforms by the separation of the signal into single reflections. This waveform decomposition provides the positions, the pulse energy and the pulse width of each reflection. Practically, this way leads to a denser point cloud in the forest area since basically each reflection – even of small tree structures below the dominant trees like young regeneration – can be detected (Jutzi and Stilla, 2006; Reitberger et al., 2008a). Note that conventional first/last pulse have a dead zone of about 3 m in which no reflection can be recorded. Moreover, the laser points get the attributes pulse energy and pulse width which are a function of object characteristics like the reflectivity and the cross section (Wagner et al., 2006). Thus, the challenge is to improve existing approaches or to develop new methods for forest structure analysis by using the dense laser point cloud and taking advantage of the additional attributes of the laser points.

New approaches to forest inventory utilizing LIDAR data have been investigated in the past. Beside area based methods, techniques for single tree extraction from conventional first/last pulse LIDAR data have been pursued for mapping forests at the tree level and for identifying important parameters, such as tree height, crown size, crown base height, and tree species. So far, most of the techniques for single tree detection are focused on the CHM that is somehow interpolated from the highest laser points. Since the interpolation process smoothes the surface drastically neighboring trees cannot be separated and, hence, groups of trees are often segmented instead of single trees. However, most important, small dominated trees and young generation below the dominating trees are completely missed since they are not visible in the CHM. The methods presented by Hyypä et al. (2001), Solberg et al. (2006) or Brandtberg (2007) are mentioned representatively. Tree species classification techniques using solely LIDAR data are mainly dedicated to the use of the laser point cloud and – very rarely – the intensity. Holmgren et al. (2004) showed that the coniferous tree species Norway spruce and Scots pine can be classified with an overall accuracy of 95% using highly dense first/last pulse LIDAR data and the non-calibrated intensity. The study of Heurich (2006) demonstrates that the classification of Norway spruce and European beech is possible with an overall accuracy of 97% in leaf-off situation using segments captured from leaf-on data. Very interestingly, although the study uses first/last pulse LIDAR data with a rather high point density of 10 points/m² it clearly points out that young regeneration could not be detected. Thus, since almost all the studies refer to conventional first/last pulse LIDAR data it is highly interesting in how far new or improved methods for single tree segmentation and tree species classification can benefit from full waveform LIDAR data.

In this paper we demonstrate how the new full waveform technique outperforms the conventional first/last pulse technique in single tree segmentation and tree species classification. The objective of this paper is (i) to shortly highlight a new segmentation method based on normalized cut that extracts single trees clearly better than the watershed segmentation, (ii) to demonstrate the improved detection rate of single trees, (iii) to prove the benefit of full waveform data both in leaf-on and leaf-off situation at different point densities, and (iv) to present classification results of deciduous and coniferous trees.

METHODS

Waveform decomposition

A single waveform measured in a region of interest (ROI) is decomposed by fitting a series of Gaussian pulses to the waveform which contains N_R reflections (Figure 1). Each reflection i of the waveform is represented by the vector $\mathbf{X}_i^T = (x_i, y_i, z_i, W_i, I_i)$ ($i = 1, \dots, N_R$) with (x_i, y_i, z_i) as the 3D coordinates, W_i as the pulse width and I_i as the pulse energy of the reflection. It is particularly remarkable that basically each reflection can be detected by the waveform decomposition contrary to conventional LIDAR Systems having a dead zone of about 3 m. These systems are effectively blind within this zone after a reflection. The parameter I_i is usually referred to as the so-called intensity. A calibration of the values W_i and I_i is mandatory and is achieved by using the pulse width and the intensity of the emitted Gaussian pulse. Additionally, the intensity I_i is corrected with respect to the run length of the laser beam and a nominal distance (Reitberger et al., 2008a; Wagner et al., 2006).

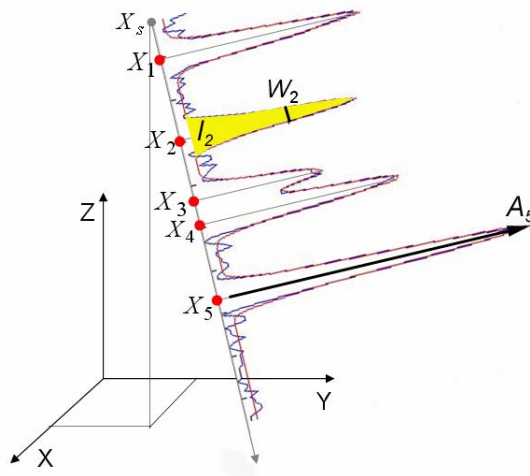


Figure 1. 3D points and attributes derived from a single waveform

Normalized cut segmentation

The key idea of the new 3D segmentation technique is to rigorously apply a normalized cut segmentation (Shi and Malik, 2000) in a voxel space. All the CHM based segmentation methods suffer from the drawback that the CHM is interpolated by some kind of interpolation process and, hence, neighbouring trees are often not separated and form a tree group instead of single trees. Moreover, smaller trees in the intermediate and lower tree height level cannot be recognized since they are invisible in the CHM (Figure 2a).

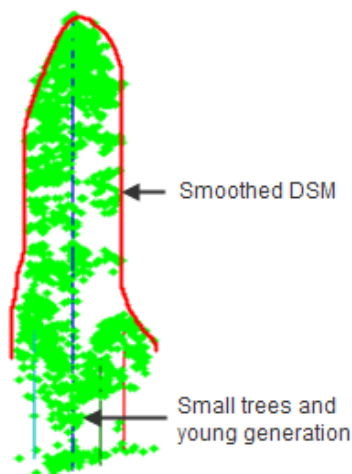


Fig. 2a. Conventional tree segmentation based on a DSM

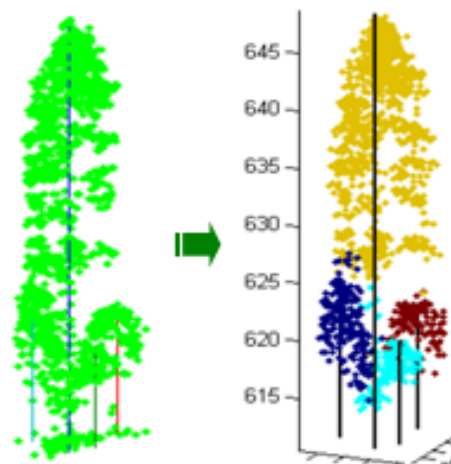


Fig. 2b. 3D segmentation of single trees

Instead, the novel 3D segmentation starts from a voxel representation of the forest area using the positions (x_i, y_i, z_i) of the reflections and optionally the pulse width W_i and the intensity I_i of the waveform decomposition (Figure 2b) (Reitberger et al., 2008b). Additionally, stem positions provided either by a special stem detection method or by a watershed segmentation of the CHM can be used.

The normalized cut segmentation applied in the voxel structure of a ROI is based on a graph G . The two disjoint segments A and B of the graph are found by maximizing the similarity of the segment members and minimizing the similarity between the segments A and B (Figure 3a) solving the cost function

$$NCut(A,B) = \frac{Cut(A,B)}{Assoc(A,V)} + \frac{Cut(A,B)}{Assoc(B,V)} \quad (1)$$

with $Cut(A,B) = \sum_{i \in A, j \in B} w_{ij}$ as the total sum of weights between the segments A and B and $Assoc(A,V) = \sum_{i \in A, j \in V} w_{ij}$ as the sum of the weights of all edges ending in the segment A. The weights w_{ij} specify the similarity between the voxels and are a function of the LIDAR point distribution and features calculated from W_i and I_i . A minimum solution for (1) is found by means of a corresponding generalized eigenvalue problem (Reitberger et al., 2008b). It turned out that the spatial distribution of the LIDAR points mainly influences the weighting function. The features derived from the LIDAR points attributes from W_i and I_i only support in second instance the segmentation result. Furthermore, we found that pre-knowledge about the position of the single tree significantly backs the segmentation. Thus, the local maxima of a CHM as a result of a watershed segmentation or stem positions – provided by a special stem detection technique (Reitberger et al., 2007) – improve the weighting function and, hence, the segmentation result. Note that the approach is not dependent from full waveform LIDAR data. It can also successfully be applied to conventional LIDAR data just providing 3D point coordinates. The figure 3b shows complex situations where the normalized cut segmentation works excellent and a conventional watershed segmentation fails.

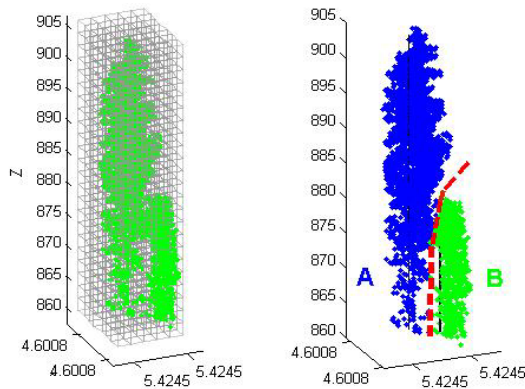


Fig. 3a. Subdivision of ROI into a voxel structure and division of voxels into two tree segments

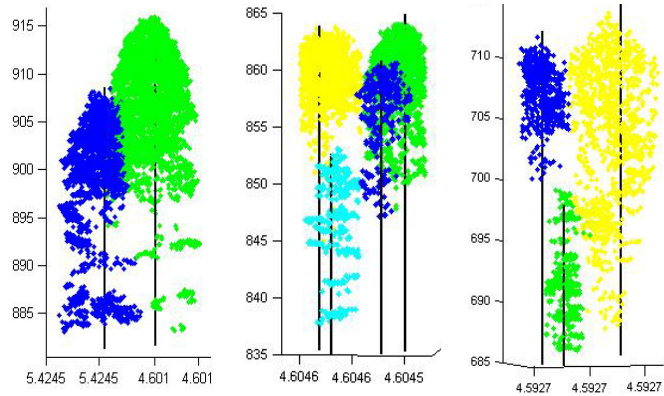


Fig. 3b. Examples of normalized cut segmentation with the reference trees as black vertical lines

Classification

We introduce for the tree species classification four groups of salient features $S_i = \{S_g, S_l, S_w, S_n\}$ which are calculated from the N_l LIDAR points $X_i^T = (x_i, y_i, z_i, W_i, I_i)$ ($i = 1, \dots, N_l$) in the segments. Table 1 summarizes the definition of the individual features (see details Reitberger et al., 2008a).

Table 1. Definition of saliencies (“Sal.”) used in classification

| Sal. | Definition | Sal. | Definition |
|-------|---|-------|--|
| s_g | Mean horizontal distances of layer points to tree trunk | s_w | Mean pulse width of single and first reflections in the entire tree segment |
| s_l | Mean intensity in entire tree | s_n | Relation of the number of single reflections to the number of multiple reflections |

Both an unsupervised and a supervised classification are performed in order to identify coniferous and deciduous tree species. The Expectation-Maximization algorithm (Heijden et al., 2004) turned out as suitable for an unsupervised clustering into the main tree species. The supervised classification was a maximum likelihood classification using an appropriate number of reference trees as a training subset (see details Reitberger et al., 2008c).

DATASET

Experiments were conducted in the Bavarian Forest National Park (49° 3' 19" N, 13° 12' 9" E), which is located in South-Eastern Germany along the border to the Czech Republic. There are four major test sites of size between 591 ha and 954 ha containing sub alpine spruce forest, mixed mountain forest and alluvial spruce forest as the three major forest types.

18 sample plots with an area size between 1000 m² and 3600 m² were selected in two test sites E and C. Reference data for all trees with DBH larger than 10 cm have been collected for 688 Norway spruces (*Picea abies*), 812 European beeches (*Fagus sylvatica*), 70 fir trees (*Abies alba*), 71 Sycamore maples (*Acer pseudoplatanus*), 21 Norway maples (*Acer platanoides*) and 2 lime trees (*Tilia Europaea*). Tree parameters like the DBH, total tree height, stem position and tree species were measured and determined by GPS, tacheometry and the 'Vertex III' system. Furthermore, the trees are subdivided into 3 layers with respect to the top height h_{top} of the plot, where h_{top} is defined as the average height of the 100 highest trees per ha (Heurich, 2006). The lower layer contains all trees below 50% of h_{top} , the intermediate layer refers to all trees between 50% and 80% of h_{top} , and finally, the upper layer contains the rest of the trees.

LIDAR data of several ALS campaigns are available for the test sites. First/last pulse data have been recorded by TopoSys with the Falcon II system. Full waveform data have been collected by Milan Flug GmbH with the Riegl LMS-Q560 system. Table 2 contains details about the point density, leaf-on and leaf-off conditions during the flights and the footprint size. The term point density is referring to the nominal value influenced by the pulse repetition frequency (PRF), flying height, flying speed and strip overlap. These unique data sets allow the comparison of conventional and full waveform systems, which have been flown in the same area. However, the data set IV is only available for the 12 reference plots in test site E. This has to be considered when comparing results of other data sets with this data set. Naturally, the reference data have been updated for the individual flying dates. Furthermore, reference trees are plotted in the figures 2a, 2b and 3b as black vertical lines.

Table 2. Different ALS campaigns

| Time of flight | Sept. '02 | May '06 | May '07 | May '07 |
|--------------------|-------------------|----------------|----------------|----------------|
| Data set | I | II | III | IV |
| Foliage | Leaf-on | Leaf-off | Leaf-on | Leaf-on |
| Scanner | TopoSys Falcon II | Riegl LMS-Q560 | Riegl LMS-Q560 | Riegl LMS-Q560 |
| Pts/m ² | 10 | 25 | 25 | 10 |
| HAAT [m] | 850 | 400 | 400 | 500 |
| Footprint [cm] | 85 | 20 | 20 | 25 |
| Ref. plots | all | All | all | Area E |

EXPERIMENTS

Segmentation

The watershed segmentation ('W') and the new 3D segmentation technique ('Ncut'), using both results from the watershed segmentation and from the stem detection, were applied to all the plots and data sets in a batch procedure without any manual interaction (Table 3). The tree positions from the segmentation are compared with reference trees if (i) the distance to the reference tree is smaller than 60% of the mean tree distance of the plot and (ii) the height difference between h_{tree} and the height of the reference tree is smaller than 15% of h_{top} . If a reference tree is assigned to more than one tree position, the tree position with the minimum distance to the reference tree is selected. Reference trees that are linked to one tree position are so-called 'detected trees' and reference trees without any link to a tree position are treated as 'non-detected' trees.

If we focus on data set II, we can highlight how the 3D segmentation is superior to the 2D watershed segmentation. The 2D segmentation performs in this case rather poor in the lower forest layer and detects almost no trees. In total, it ends up at an overall detection rate of 48 %. Instead, the detection rate of the novel 3D segmentation is by 16 % better in the lower and intermediate layer. Even in the upper layer the improvement is 10 %, whereas the overall detection rate increases by 12 %. Apparently, the waveform decomposition detects not only the reflections of the dominant trees but also of the dominated small trees. The 3D segmentation takes full advantage of this and yields clearly better segmentation results.

Now, let us compare the segmentation methods with respect to first/last pulse data (data set I) and to full waveform data (data set IV) at the same nominal point density. First, even the 2D watershed based segmentation performs by 5 % better with full waveform data. Obviously, the tree shapes are more precisely reconstructed since the waveform decomposition even yields weak reflections and reflections resulting from adjacent targets. However, most important, the combination of the full waveform data with the new 3D segmentation improves the detection rate by more than 20 % in the lower and intermediate layer. This is a remarkable progress and finds its interpretation in the high spatial point distribution the waveform decomposition provides and the new segmentation working fully in 3D rather than to apply the segmentation on the CHM.

Table 3. Results of segmentation methods with data sets I, II, III and IV

| Data set | Method | Detected trees per height layer [%] | | | |
|-------------------|--------|-------------------------------------|--------------|-------|-------|
| | | lower | intermediate | upper | total |
| I (only area E) | W | 2 | 12 | 80 | 52 |
| | NCut | 15 | 27 | 77 | 55 |
| II | W | 5 | 21 | 77 | 48 |
| | NCut | 21 | 38 | 87 | 60 |
| III | W | 5 | 20 | 79 | 48 |
| | NCut | 17 | 32 | 86 | 58 |
| III (only area E) | W | 5 | 20 | 82 | 55 |
| | NCut | 24 | 35 | 88 | 66 |
| IV (only area E) | W | 6 | 21 | 84 | 57 |
| | NCut | 26 | 33 | 87 | 65 |

This unique data set also demonstrates the impact of the nominal point density on the segmentation methods. If we restrict data set III to the area E and compare it with data set IV we recognize that the detection rates are basically the same for both point densities. Obviously, although the number of penetrating laser beams is significantly reduced, the most relevant tree structures are still detected by reflections.

Finally, we can also address the question whether the foliage condition affects the detection rate if we compare the full waveform data sets II (leaf-off) and data set III (leaf-on). As expected, the detection rate is in leaf-on situation by approximately 4 % worse in the lower and intermediate layer. But in the upper layer the results of the normalized cut segmentation are almost equal, leading to an overall loss of accuracy of 2 % in leaf-on situation.

Classification

We apply an unsupervised and a supervised classification between deciduous and coniferous trees to the 2D segments (Table 4) and 3D segments (Table 5). One fifth of the trees were randomly selected from the entire data set as a training data set for the supervised classification by keeping the proportion between the tree species. Also, both classification methods were applied 20 times in order to minimize the impact of the selection procedure and the initialization of the EM-algorithm of the unsupervised classification on the results. Thus, the numbers in table 4 and table 5 refer to averaged classification values, whereby the best result of each data set and classification method is highlighted.

In general, if we focus on the best results of each saliency the supervised classification turns out as slightly better than the unsupervised classification. Furthermore, the classification results are almost the same for the 2D segments and 3D segments. Apparently, the applied saliencies and their combinations are highly characteristic both for the dominant trees in the upper layer and for the dominated trees in the lower and intermediate layer. Moreover, except for the tree shape related saliency S_g it is not relevant whether one or more trees of the same tree species are in one segment.

Most interestingly, the intensity related saliency S_I turns out as the best feature in the leaf-on case (data sets III and IV). As expected, this feature is worse in the leaf-off case. Instead, the saliency S_n dedicated to penetration behavior of the waveforms influences the classification results significantly in the leaf-off case (data set II). The saliency S_w dedicated to the pulse width of the reflections works in general better in the leaf-off case. Finally, the

saliency S_g representing the tree geometry has an almost constant impact on the classification in leaf-on and leaf-off situations. Even for data set I, which refers to first/last pulse data at a point density of 10 pts/m², the overall classification accuracy is almost the same as with full waveform data. Thus, this saliency seems to be significant even for the lower point density.

Table 4. Results of unsupervised („un.“) and supervised classification („su.“)

| Saliency | Overall accuracy (%) for data sets I - IV and for the 2D segments | | | | | | | | | |
|-------------------------|--|-----|----------|-----|---------|-----|-------------------|-----|------------------|-----|
| | I (only area E) | | II | | III | | III (only area E) | | IV (only area E) | |
| | Leaf-on | | Leaf-off | | Leaf-on | | Leaf-on | | Leaf-on | |
| | un. | su. | un. | su. | un. | su. | un. | su. | un. | su. |
| S_g | 84 | 85 | 79 | 83 | 85 | 85 | 82 | 85 | 82 | 83 |
| S_l | | | 82 | 81 | 92 | 93 | 96 | 95 | 95 | 96 |
| S_w | | | 81 | 82 | 52 | 53 | 54 | 55 | 56 | 61 |
| S_n | | | 86 | 94 | 65 | 65 | 64 | 65 | 54 | 64 |
| $S_g + S_l$ | | | 89 | 90 | 92 | 94 | 94 | 97 | 93 | 97 |
| $S_g + S_l + S_w + S_n$ | | | 92 | 96 | 83 | 95 | 82 | 97 | 83 | 97 |

Table 5. Results of unsupervised („un.“) and supervised classification („su.“)

| Saliency | Overall accuracy (%) for data sets I - IV and for the 3D segments | | | | | | | | | |
|-------------------------|--|-----|----------|-----|---------|-----|-------------------|-----|------------------|-----|
| | I (only area E) | | II | | III | | III (only area E) | | IV (only area E) | |
| | Leaf-on | | Leaf-off | | Leaf-on | | Leaf-on | | Leaf-on | |
| | un. | su. | un. | su. | un. | su. | un. | su. | un. | su. |
| S_g | 80 | 78 | 75 | 78 | 80 | 82 | 83 | 82 | 81 | 81 |
| S_l | | | 81 | 81 | 93 | 94 | 97 | 96 | 95 | 97 |
| S_w | | | 75 | 79 | 52 | 51 | 54 | 56 | 60 | 64 |
| S_n | | | 89 | 93 | 62 | 63 | 61 | 65 | 57 | 57 |
| $S_g + S_l$ | | | 81 | 86 | 90 | 94 | 93 | 97 | 91 | 97 |
| $S_g + S_l + S_w + S_n$ | | | 91 | 94 | 81 | 95 | 84 | 97 | 82 | 97 |

As far as the foliage condition is concerned, data sets II and III show equal classification accuracies, where the significance of the individual saliencies is different. Furthermore, the point density has almost no impact on the classification results, if we focus on data set III (only area E) and data set IV (only area E). This is fully consistent with our observation that also the segmentation is not dependent on the point density. Thus, the lower point density of 10 pts/m² does not appear as disadvantageous. Finally, the comparison of data set I (only area E) and data set IV (only area E), which both refer to leaf-on situation and a nominal point density of 10 pts/m², indicates that the classification with first/last pulse data is significantly inferior by about 15% since only the coordinates of the reflections could be used and hence, the saliency S_g could only be calculated for the classification.

DISCUSSION

The experiences clearly prove that the new segmentation working in 3D can be viewed as a breakthrough for single tree segmentation. If this method is combined with full waveform LIDAR data the detection rate of single trees is improved by more than 20 % in the lower forest layers. Our experiments demonstrate that the usage of full waveform data is clearly superior to first/last pulse data in wooded areas since the waveform decomposition finds almost all reflections. Thus, small dominated trees and young generation can be detected and highly resolved. In detail, we got a slightly higher detection rate in leaf-off situation because of the higher penetration in unfoliated

deciduous trees. Thus, the leaf-off situation seems to be the more appropriate flying time to segment trees in 3D, at least for mixed mountain forests that are scanned with a high point density. Interestingly, a nominal point density higher than 10 pts/m² does not improve the detection rate considerably. However it remains to be seen whether a higher density is advantageous to estimate other parameters like for instance the timber volume. Finally, our results with the watershed segmentation compare reasonably well with the study of Heurich (2006), who obtained an overall detection rate of 45% in almost the same reference areas using also the data set I. The study of Persson et al. (2002) reports on a detection rate of 71 % of all trees with a diameter at breast height larger than 5 cm for a Scandinavian forest dominated by spruce and pine. Solberg et al. (2006) show that an overall detection rate of 66 % and a commission rate (=false detections) of 26 % in a structurally heterogeneous spruce forest can be achieved if the CHM is smoothed 3 times with a Gaussian filter of size 30 cm.

When viewing at the classification results the benefit of full waveform LIDAR data becomes more evident since the overall accuracy is significantly increased. In case of the supervised classification we attained an overall accuracy of 95 % for all reference data, the unsupervised classification is only slightly inferior. Moreover, the results are practically independent on the point density and the foliage condition. All in all, the improved detection rate of single trees leads to an increased number of correctly classified trees. For instance, a detection rate of 60 % and a classification accuracy of 94 % imply 56 % correctly detected and classified trees. Finally, our classification results of 80 % overall accuracy with first/last pulse data in leaf-on case compare excellent with the experiments of Heurich (2006). However, our results with the full waveform data in leaf-on situation are in any classification case better than the leaf-on results with first/last pulse data of this study.

CONCLUSIONS

We have shown in this study how a new 3D segmentation technique clearly outperforms conventional segmentation methods which solely work with the CHM. Furthermore, the combination with full waveform LIDAR data pushes the detection rate to a significantly improved success rate. Also, the classification accuracy of single coniferous and deciduous trees based on 3D segments is considerably enhanced using full waveform LIDAR data.

REFERENCES

- Brandtberg, T., 2007. Classifying individual tree species under leaf-off and leaf-on conditions using airborne lidar. *ISPRS Journal of Photogrammetry and Remote Sensing*, 61, pp. 325 – 340.
- Heijden, F. van der, Duin, R.P.W., Ridder, D. de and Tax, D.M.J., 2004, Classification, parameter estimation and state estimation – An engineering approach using MATLAB. John Wiley & Sons Ltd, The Atrium, southern Gate, Chichester, West Sussex PO19 8SQ, England
- Heurich, M., 2006. Evaluierung und Entwicklung von Methoden zur automatisierten Erfassung von Waldstrukturen aus Daten flugzeuggetragener Fernerkundungssensoren. Forstlicher Forschungsbericht München, Nr. 202, ISBN 3-933506-33-6. <http://meadiatum2.ub.tum.de/>. (Accessed December 16, 2008).
- Holmgren, J., Persson, Å., 2004, Identifying species of individual trees using airborne laser scanner. *Remote Sensing of Environment* 90 (2004) 415 – 423.
- Hyypä, J., Kelle, O., Lehtikoinen, M., Inkinen, M., 2001. A segmentation-based method to retrieve stem volume estimates from 3-D tree height models produced by laser scanners. *IEEE Transactions on Geoscience and Remote Sensing*, 39: 969 – 975.
- Jutzi, B., Stilla, U., 2006. Range determination with waveform recording laser systems using a Wiener Filter. *ISPRS Journal of Photogrammetry and Remote Sensing*, 61, pp. 95 – 107.
- Kötz, B., 2006. Estimating biophysical and biochemical properties over heterogeneous vegetation canopies - Radiative transfer modeling in forest canopies based on imaging spectrometry and LIDAR. Dissertation, ETH Zürich. <http://www.dissertationen.unizh.ch/2006/koetz/diss.pdf>. (Accessed December 16, 2008).
- Mallet, c., Bretar, F., 2008. Full-waveform topographic lidar: State-of-the-art. *ISPRS Journal of Photogrammetry and Remote Sensing* (in press).

- Morsdorf, F., Nichol C., Malthus T.J., Patenaude G., Woodhouse, I.H., 2008. Modelling multi-spectral LIDAR vegetation backscatter – assessing structural and physiological information content. *SilviLaser 2008*, Sept. 17-19, Edinburgh, UK.
- Reitberger, J., Krzystek, P., Stilla, U., 2007. Combined tree segmentation and stem detection using full waveform LIDAR data. *Proceedings of the ISPRS Workshop Laser Scanning 2007 and SilviLaser 2007*, Volume XXXVI, PART 3/W52, 12 – 14th September 2007, Espoo, pp. 332 – 337.
- Reitberger, J., Krzystek, P., Stilla, U., 2008a. Analysis of full waveform LIDAR data for the classification of deciduous and coniferous trees. *International Journal of Remote Sensing*. Vol. 29, No. 5, March 2008 , pp. 1407 – 1431.
- Reitberger, J., Schnörr, Cl., Krzystek, P., Stilla, U., 2008b. 3D segmentation of full waveform LIDAR data for single tree detection using normalized cut. *IAPRS Vol. XXXVII, Part B3a*, 3 – 11th July 2008, Beijing, pp. 77 – 83.
- Reitberger, J., Krzystek, P., Stilla, U., 2008c. 3D segmentation and classification of single trees with full waveform LiDAR data. *Proceedings of SilviLaser 2008, 8th international conference on LiDAR applications in forest assessment and inventory*, Edinburgh, UK, pp. 216 – 226.
- Persson, A., Holmgren, J. and Söderman, U., 2002. Detecting and measuring individual trees using an airborne laserscanner. *Photogrammetric Engineering & Remote Sensing* 68(9), pp. 925–932
- Shi, J., Malik, J., 2000. Normalized cuts and image segmentation. *IEEE Transactions on Pattern Analysis and Machine Intelligence*, 22, pp. 888 – 905.
- Solberg, S., Naesset, E., Bollandsas, O. M., 2006. Single Tree Segmentation Using Airborne Laser Scanner Data in a Structurally Heterogeneous Spruce Forest. *Photogrammetric Engineering & Remote Sensing*, Vol. 72, No. 12, December 2006, pp. 1369 – 1378.
- Sun, G., Ranson, K.J. 2000. Modeling Lidar Returns from Forest Canopies. *IEEE Transactions on GeoScience and Remote Sensing*. Vol. 38, NO. 6, November.
- Wagner, W., Ullrich, A., Ducic, V., Melzer, T., Studnicka, N., 2006. Gaussian decomposition and calibration of a novel small-footprint full-waveform digitising airborne laser scanner. *ISPRS Journal of Photogrammetry and Remote Sensing*, 60, pp. 100 – 112.